The behaviour of high Reynolds flows in a driven cavity

Charles-Henri BRUNEAU and Mazen SAAD

Mathématiques Appliquées de Bordeaux, Université Bordeaux 1
CNRS UMR 5466, INRIA team MC^2
351 cours de la Libération, 33405 Talence, France
Charles-Henri.Bruneau@math.u-bordeaux1.fr, Mazen.Saad@math.u-bordeaux1.fr

Abstract

Numerical simulations of the 2D lid-driven cavity flow are performed at high Reynolds number $Re = 100000$. The qualitative behaviour of the turbulent solution at this high Reynolds number is described and analyzed with respect to the time scheme and the grid. Global quantities such as the energy and the enstrophy show that solutions computed from a different initial datum converge to the same asymptotic stage as expected due to the existence of a global attractor.

Keywords: Navier-Stokes equations; Lid-driven cavity problem; High Reynolds flows

1 Introduction

In the eighties' a lot of theoretical works were dedicated to the existence of exponential attractors for dissipative evolution equations (see [2] and references therein). In particular many researches concern the two dimensional Navier-Stokes equations for which an estimate on the upper bound of the attractor dimension was obtain [8]. Although it is still difficult to compute reliable solutions of these equations at high Reynolds numbers, it seems possible to get a qualitative behaviour of the solutions. The aim of this work is both to give some transient solutions at $Re = 100000$ in the lid-driven cavity problem and to give a numerical confirmation of the presence of an attractor starting with two very different initial data. There are very few computations at such a high Reynolds number in the literature as it is difficult to represent correctly the flow in the boundary layer. Nevertheless in [6] some results give a view of the solution in the transient starting from rest.

The numerical simulation lie on a finite differences discretization and on a multigrid solver with a cell-by-cell relaxation procedure. Classical Euler or Gear time schemes with explicit treatment of convection terms are coupled to a second-order approximation of the linear terms in space and a third order scheme for nonlinear terms [1]. To get reliable results the solutions with the multigrid algorithm are computed on finest grids as fine as possible and the results are analysed on various global quantities. Although finest 1024×1024 and 2048×2048 cells grids are used, the aim of this paper is not to give benchmark results but to study the qualitative behaviour of the solutions. On the one hand the solutions in the transient are described for the two grids and the two time schemes. And on the other hand it is shown that the solutions computed from two different initial data converge to the same asymptotic stage as expected by the existence of an attractor for two dimensional Navier-Stokes equations.

In the next section the Navier-Stokes equations in primitive variables are recalled and an outline of the computational method is given. Then the numerical results are carefully analysed.

2 Governing equations and discretization

To solve the incompressible flow in a 2D square cavity $\Omega = (0,1) \times (0,1)$ and for a time interval $(0,T)$, we set the unsteady Navier-Stokes equations:

$$\left\{ \begin{array}{rcll} \partial_t U - \dfrac{1}{Re}\Delta U + (U \cdot \nabla)U + \nabla p &=& 0 & \text{in }]0,T[\times\Omega \\ \nabla \cdot U &=& 0 & \text{in }]0,T[\times\Omega \\ U(t,x,y) &=& (-1,0) & \text{on }]0,T[\times\Gamma_1 \\ U(t,x,y) &=& (0,0) & \text{on }]0,T[\times\Gamma_0 \\ U(0,x,y) &=& U_0(x,y) & \text{in } \Omega \end{array} \right. \tag{1}$$

where $U = (u,v)$ and p are respectively the velocity and the pressure, Γ_1 is the top boundary, Γ_0 represents the three other sides and U_0 is an initial datum. The system of equations (1) is discretized by means of either a first order Euler scheme or a second order Gear scheme. The linear terms are treated implicitly whereas the convection terms are treated explicitly. Let U^n be the approximation of U at time $t_n = n\delta t$, the Euler semi-discretized system reads :

$$\left\{ \begin{array}{rcll} \dfrac{U^n}{\delta t} - \dfrac{1}{Re}\Delta U^n + \nabla p^n &=& \dfrac{U^{n-1}}{\delta t} - (U^{n-1} \cdot \nabla)U^{n-1} & \text{in } \Omega \\ \nabla \cdot U^n &=& 0 & \text{in } \Omega \\ U^n &=& (-1,0) & \text{on } \Gamma_1 \\ U^n &=& (0,0) & \text{on } \Gamma_0 \end{array} \right. \tag{2}$$

and the Gear semi-discretized system reads :

$$\left\{ \begin{array}{rcll} \dfrac{3U^n}{2\delta t} - \dfrac{1}{Re}\Delta U^n + \nabla p^n &=& \dfrac{2U^{n-1}}{\delta t} - 2(U^{n-1} \cdot \nabla)U^{n-1} & \\ & & -\dfrac{U^{n-2}}{2\delta t} + (U^{n-2} \cdot \nabla)U^{n-2} & \text{in } \Omega \\ \nabla \cdot U^n &=& 0 & \text{in } \Omega \\ U^n &=& (-1,0) & \text{on } \Gamma_1 \\ U^n &=& (0,0) & \text{on } \Gamma_0 \end{array} \right. \tag{3}$$

We shall see on numerical results the influence of the time scheme to the transient behaviour.
The system of equations (2) or (3) is discretized in space by finite differences on an uniform staggered grid. The discrete values of the pressure are located at the center of each cell and those of the velocity field are located at the middle of the sides as shown on figure 1.

The discretization of the left hand side of equations (2) or (3) is achieved using second or-

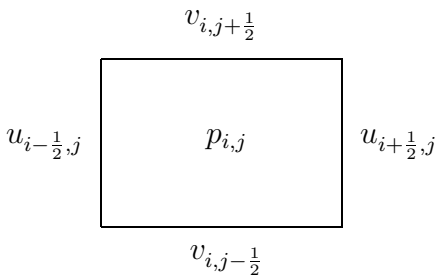

Figure 1: A staggered cell

der centered finite differences. For instance, the divergence-free equation is approximated at the pressure point (i, j) by

$$\frac{u^n_{i+\frac{1}{2},j} - u^n_{i-\frac{1}{2},j}}{\delta x} + \frac{v^n_{i,j+\frac{1}{2}} - v^n_{i,j-\frac{1}{2}}}{\delta y} = 0.$$

in order to link the four velocity components of the same cell. The convection terms in the right hand side of equations (2) are approximated by the third order scheme constructed in [1]. For instance the discretization of the term $-v^{n-1}\partial_y u^{n-1}$ at point $(i - \frac{1}{2}, j)$ (see figure 1) is given by

$$\begin{array}{ll} -\frac{1}{3}v^{n-1}_{i-\frac{1}{2},j+\frac{1}{2}}\frac{\Delta_{i-\frac{1}{2},j+\frac{1}{2}}u^{n-1}}{\delta y} - \frac{5}{6}v^{n-1}_{i-\frac{1}{2},j-\frac{1}{2}}\frac{\Delta_{i-\frac{1}{2},j-\frac{1}{2}}u^{n-1}}{\delta y} + \frac{1}{6}v^{n-1}_{i-\frac{1}{2},j-\frac{3}{2}}\frac{\Delta_{i-\frac{3}{2},j-\frac{3}{2}}u^{n-1}}{\delta y} & \text{if } v^{n-1}_{i-\frac{1}{2},j-\frac{1}{2}} > 0 \\ -\frac{1}{3}v^{n-1}_{i-\frac{1}{2},j-\frac{1}{2}}\frac{\Delta_{i-\frac{1}{2},j-\frac{1}{2}}u^{n-1}}{\delta y} - \frac{5}{6}v^{n-1}_{i-\frac{1}{2},j+\frac{1}{2}}\frac{\Delta_{i-\frac{1}{2},j+\frac{1}{2}}u^{n-1}}{\delta y} + \frac{1}{6}v^{n-1}_{i-\frac{1}{2},j+\frac{3}{2}}\frac{\Delta_{i-\frac{3}{2},j+\frac{3}{2}}u^{n-1}}{\delta y} & \text{if } v^{n-1}_{i-\frac{1}{2},j+\frac{1}{2}} < 0. \end{array}$$

This new third-order scheme has been compared successfully in [1] to the classical ones, namely the original third-order upwind scheme, the quickest scheme [7] and an other upwind scheme based on a centered stencil [5].
To reduce the CPU time a multigrid algorithm using a V-cycle procedure and a Gauss-Seidel cell-by-cell smoother is used to solve the system at each time step.

3 Numerical results

We present here various numerical results at $Re = 100000$ performed on fine grids of 1024×1024 and 2048×2048 cells to get reliable results. The goal is to have a mesh size small enough to capture the boundary layer effects. With these fine grids, we ensure that there are a few grid points in the boundary layer. Of course, we do not claim that the number of points is sufficient to represent the whole phenomenon but is enough to get a good qualitative behaviour of the solution. In addition we compare the results obtained with the two time schemes. The first test is to compute the solution from rest on two consecutive grids for a short time. We can see on figures 2 and 3 that the solutions obtained in the transient stage look similar on the two consecutive grids even if it is clear that there is more diffusive effects with the coarser grid.

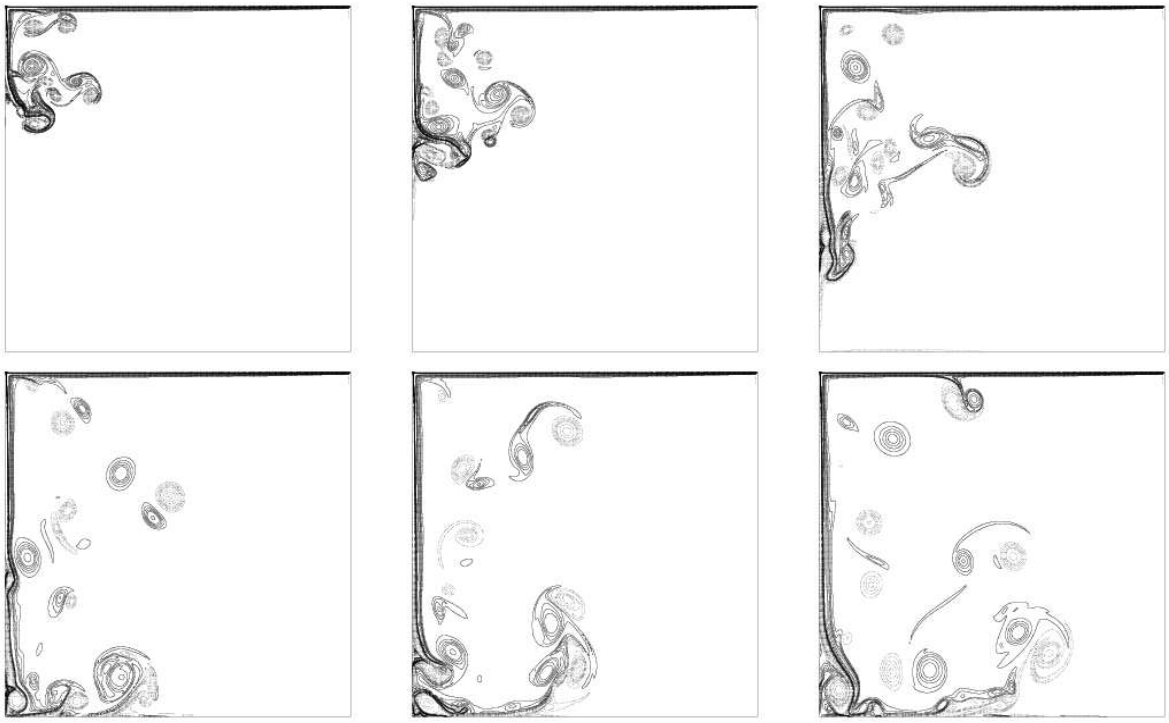

grid 1024×1024

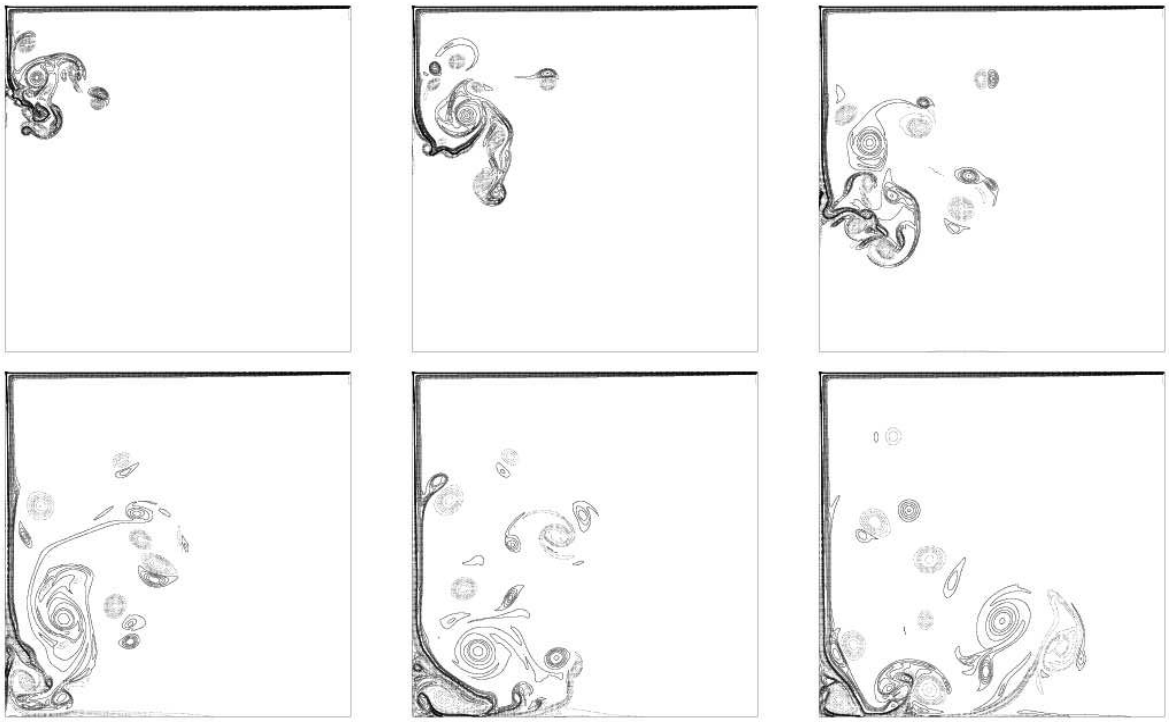

grid 2048×2048

Figure 2: Evolution of the vorticity with Euler scheme for $Re = 100000$ at times $t = 4$, $t = 6$, $t = 10$, $t = 14$, $t = 16$ and $t = 20$ (from left to right and top to bottom).

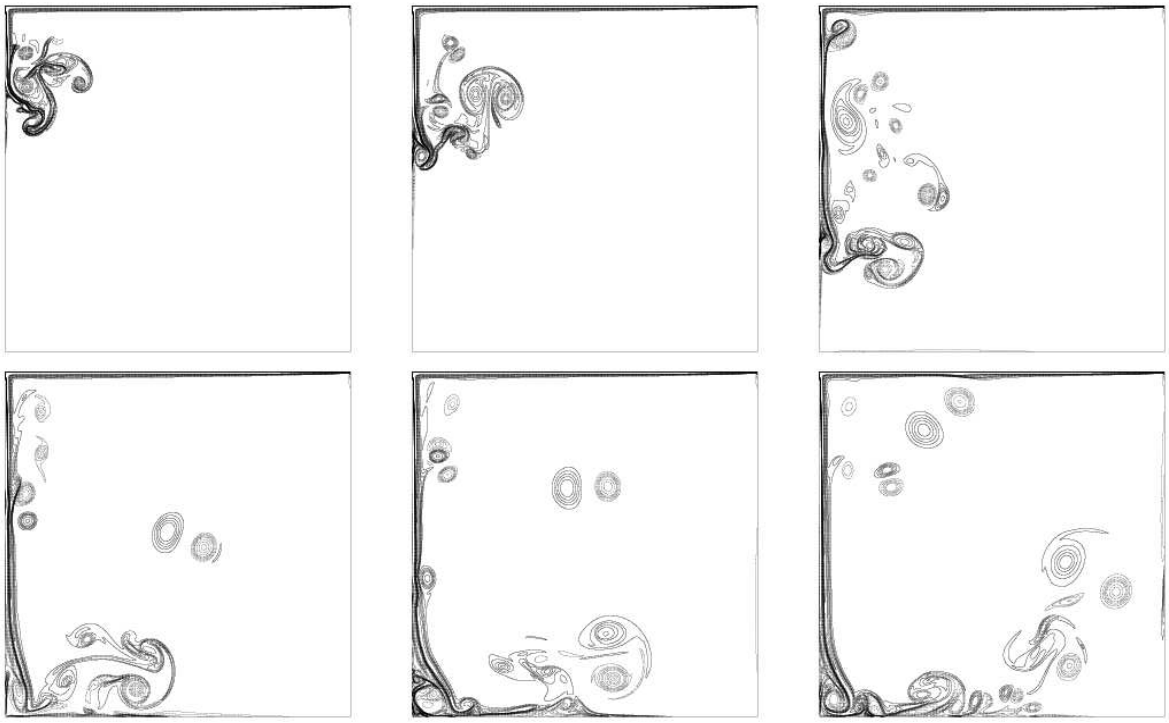

grid 1024×1024

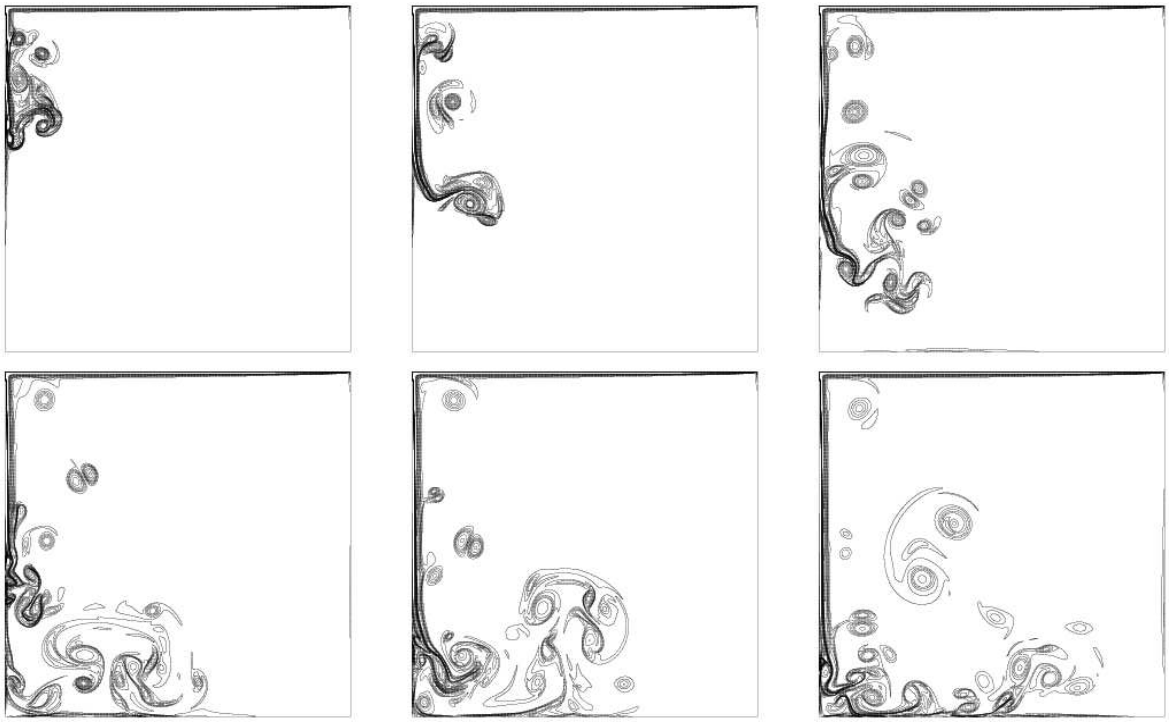

grid 2048×2048

Figure 3: Evolution of the vorticity with Gear scheme for $Re = 100000$ at times $t = 4$, $t = 6$, $t = 10$, $t = 14$, $t = 16$ and $t = 20$ (from left to right and top to bottom).

In addition the results obtained with Gear scheme are more reliable as the corresponding solution exhibits more vortices and in particular more small eddies along the wall (shown clearly at time $t = 20$). Let us point out to the reader that to better isolate the various vortices we have represented the vorticity isolines given in table 1.

The results in the transient are not similar and it is clear that the grid convergence is

	Isolines values					
Stream-function	-0.1	-0.08	-0.06	-0.04	-0.02	-0.01
	-3×10^{-3}	-1×10^{-3}	-3×10^{-4}	-1×10^{-4}	-3×10^{-5}	-1×10^{-5}
	-3×10^{-6}	-1×10^{-6}	-1×10^{-7}	-1×10^{-8}	-1×10^{-9}	-1×10^{-10}
	0.0	1×10^{-10}	1×10^{-9}	1×10^{-8}	1×10^{-7}	1×10^{-6}
	3×10^{-6}	1×10^{-5}	3×10^{-5}	1×10^{-4}	3×10^{-4}	1×10^{-3}
	3×10^{-3}	0.01	0.03	0.05	0.07	0.09
	0.1	0.11	0.115	0.1175		
Vorticity	-40.0	-35.0	-30.0	-25.0	-20.0	-15.0
	-10.0	-8.0	-6.0	-4.0	-2.0	
		2.0	4.0	6.0	8.0	10.0
	15.0	20.0	25.0	30.0	35.0	40.0
Pressure	from -2.0 to 2.0 by step 0.01					

Table 1: Contours values of the stream-function, the vorticity and the pressure.

not reached. However global quantities as the kinetic energy or the enstrophy defined by

$$E = \frac{1}{2}\int_\Omega \|U\|^2 dx, \quad Z = \frac{1}{2}\int_\Omega \|\omega\|^2 dx,$$

are identical for this short time. The problem is to compare our solutions to other simulations or experiments. Unfortunately, there is very few results available in the literature but it seems that qualitatively the behaviour of our solutions is correct. At intermediate Reynolds number $Re = 25000$, the solution exhibits about the same structures along the walls but there is still a strong primary vortex in the center of the cavity [3]. However some authors find a more regular solution at $Re = 30000$ [4]. On the contrary, at $Re = 100000$ there are many more eddy structures filling up the whole cavity as it can be seen also in [6].

In addition, to validate our results we verify that the flux term

$$\int_\Omega U \cdot (U \cdot \nabla) U dxdy$$

vanishes in the lid-driven cavity as $U \cdot n = 0$ on the boundary. As the velocity components are given on staggered grids, we evaluate the whole quantity at the center of each cell and then approximate the integral by the first order formula

$$\delta x \delta y \;\; \Sigma_{i,j} (U \cdot (U \cdot \nabla) U)_{i,j}.$$

Numerically we get a mean value in time around 6×10^{-5} on the grid 1024×1024 and around 3×10^{-5} on the grid 2048×2048.

The second numerical test is performed initializing the solution at time $t = 0$ with the steady solution obtained at $Re = 5000$ with global values $E = 0.0473$ and $Z = 40.26$ (see figure 4).

The aim of this second test is to compare the behaviour of the solution with respect to

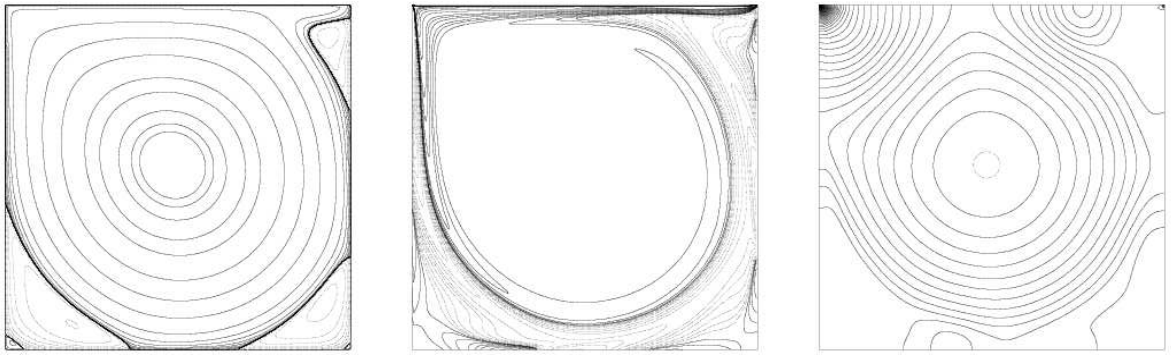

Figure 4: Steady solution at $Re = 5000$ computed with present scheme on grid 1024×1024. From left to right stream-function, vorticity and pressure fields.

the initialization. We know that for the 2D Navier-Stokes equations there is an attractor, so we expect the behaviour of the solutions is asymptotically close. The question is to estimate the time needed to reach the asymptotic state. On the one hand, the plots of figure 5 illustrate the evolution of the solution in the transient stage starting from rest. The stream-function contours at times $t = 10$, $t = 100$, $t = 200$ and $t = 400$ show that the flow enters progressively the cavity to yield a quite stable gyrator flow in the middle. Nevertheless, the vorticity and pressure isolines reveal the presence of numerous eddies coming from the walls inside the whole cavity. A careful study indicates that the effects of viscosity are confined to a thin layer close to the solid boundaries. Small eddies develop in the vicinity of the walls and the two lower corners. These eddies are sometimes organized in Karman alleys and yield dipole structures that are convected inside the cavity. This is confirmed by some animations and many pictures available on the web page *http://www.math.u-bordeaux1.fr/MAB/DNS*. A similar behaviour is shown in [6].

On the other hand, the evolution of the solution starting from the steady solution computed at $Re = 5000$ is given on figure 6. The same quantities plotted at the same times show that the strong primary vortex is progressively reduced as many eddies coming from the wall spread into the whole domain. At the beginning the three secondary vortices in the corners are broken by the small eddies. Then the two flows look much more similar as can be seen at time $t = 400$ (last line of figures 5 and 6).

This is confirmed by the energy and enstrophy histories. Indeed the energy of the first simulation increases with time from zero as the energy of the second simulation decreases from the value reached by the steady solution at $Re = 5000$ namely 0.0473 (figure 7). In addition the enstrophy histories are much more similar at the end of the numerical simulations. The asymptotic stage is not fully reached but from time $t = 300$ the solutions are quite close and become closer as time is going on. In addition the enstrophy histories are similar at the end of the simulation.

To confirm that the behaviour of both solutions is quite close, the velocity evolution from time $t = 200$ to time $t = 400$ at monitoring point (14/16,1/16) is plotted on figure 8. We

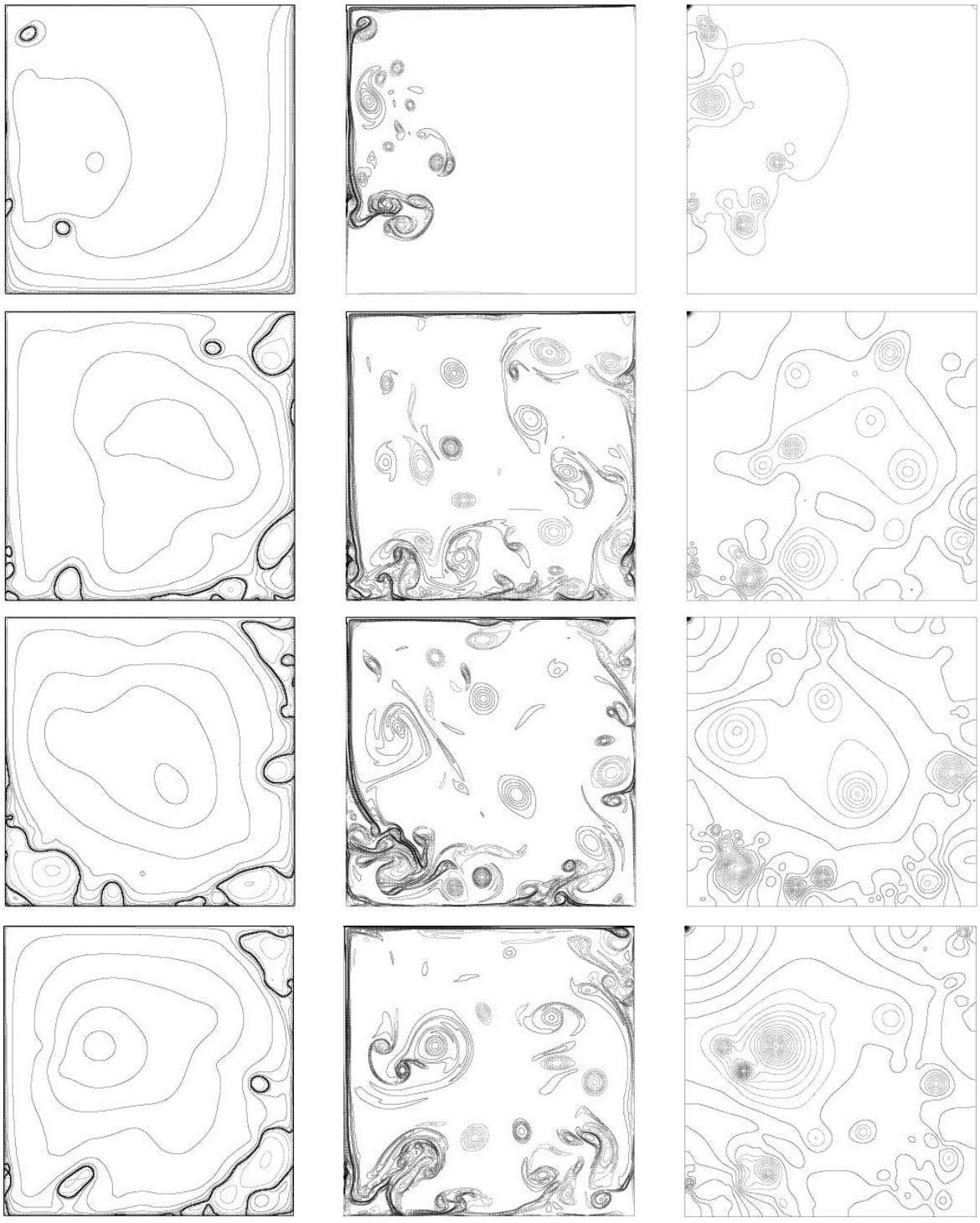

Figure 5: Evolution of the solution at $Re = 100000$ computed from initialization at rest. From left to right stream-function, vorticity and pressure fields on grid 1024×1024 at times $t = 10$, $t = 100$, $t = 200$ and $t = 400$. Computation with Gear scheme in time.

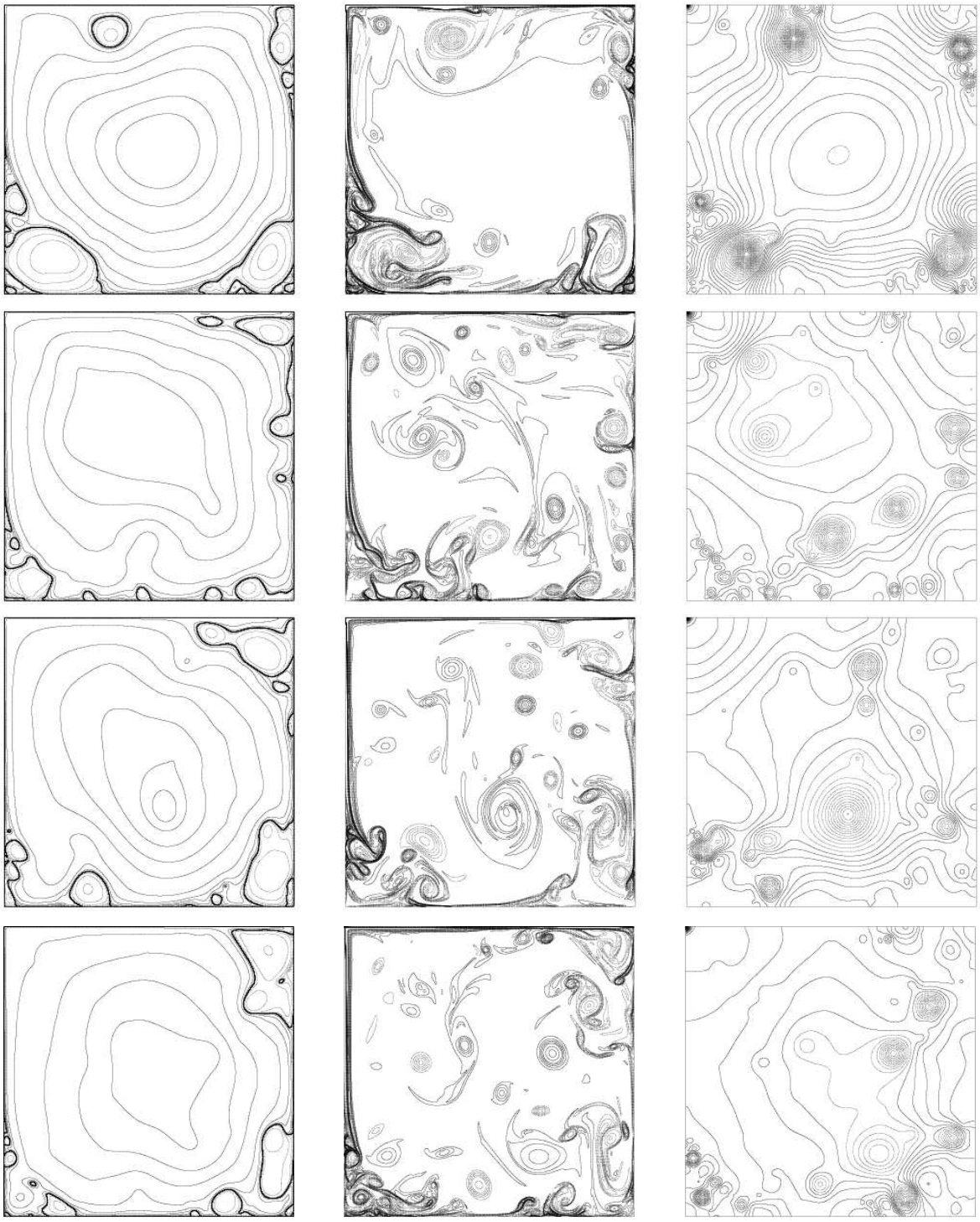

Figure 6: Evolution of the solution at $Re = 100000$ computed from initialization by the steady solution at $Re = 5000$. From left to right stream-function, vorticity and pressure fields on grid 1024×1024 at times $t = 10$, $t = 100$, $t = 200$ and $t = 400$. Computation with Gear scheme in time.

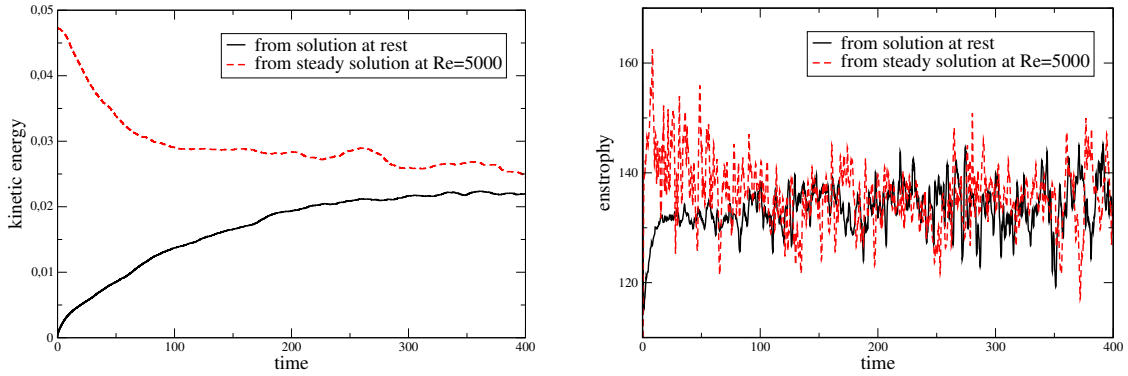

Figure 7: Comparison of the energy (left) and the enstrophy (right) histories at $Re = 100000$ with the two initializations.

see clearly that the time signals are also similar. On figure 9 is plotted the corresponding Fourier spectrum of the two signals which are quite close with respect to the frequency and the amplitude. Let us note that the two spectra of the horizontal component capture about the same main low frequency and that the two spectra of the vertical component exhibit many peaks located at about the same place.

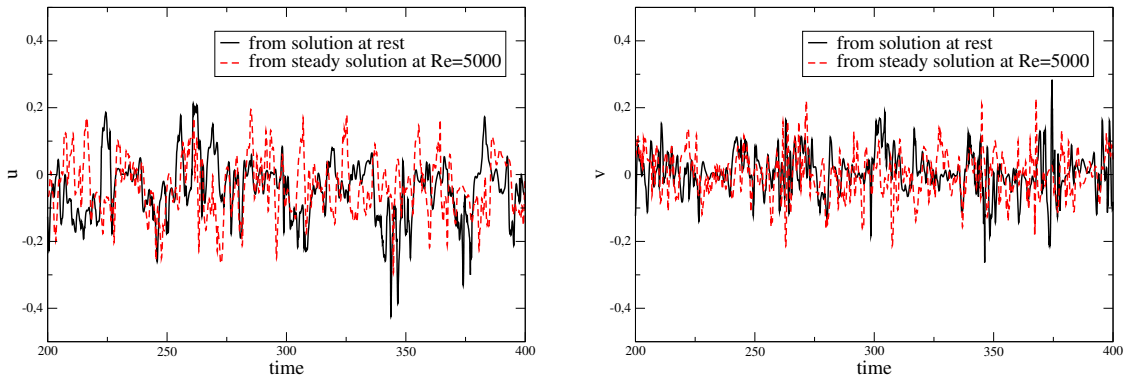

Figure 8: Horizontal (left) and vertical (right) velocity components history at monitoring point (14/16,1/16) for $Re = 100000$.

4 Conclusion

The various computations at high Reynolds number show the robustness and efficiency of the approximation and of the computational method. The direct numerical simulation of the unsteady Navier-Stokes equations with a strongly coupled solver in the primitive variables, enable to describe the qualitative behaviour of the solution at $Re = 100000$. The numerical tests from two different initial solutions converge toward the same asymptotic stage, confirming the presence of an attractor.

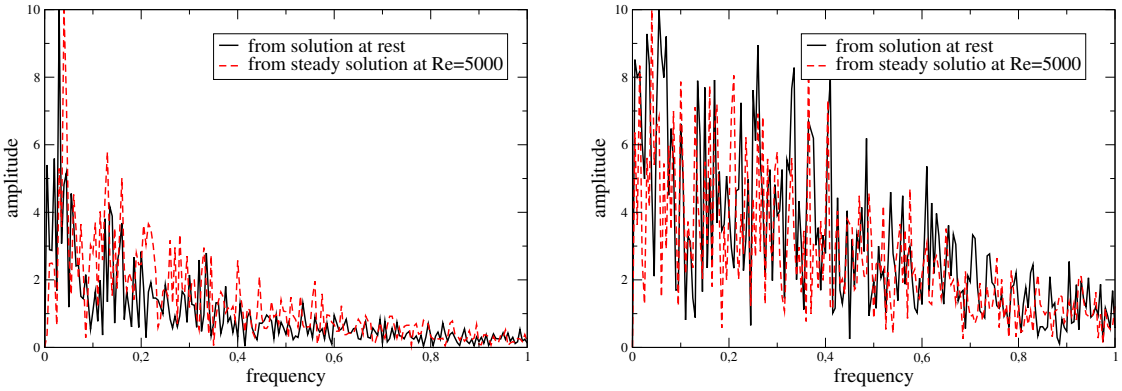

Figure 9: Power spectrum of the horizontal (left) and the vertical (right) velocity components at monitoring point (14/16,1/16) for $Re = 100000$.

References

[1] Ch.-H. Bruneau, M. Saad, *The 2D lid-driven cavity problem revisited*, Computers & Fluids **35** n° 3, 2006.

[2] A. Eden, C. Foias, B. Nicolaenko, R. Temam, *Exponential attractors for dissipative evolution equations*, Research in Applied Mathematics **37**, Masson, 1994.

[3] U. Goodrich, *An efficient and robust algorithm for two dimensional time dependent incompressible Navier-Stokes equations : High Reynolds number flows*, 7^{th} Int. Conf. Num. Meth. Laminar Turbulent Flow, Stanford, and NASA Technical Memorandum n° 104424, 1991.

[4] A. Huser, S. Biringen, *Calculation of two-dimensional shear-driven cavity flows at high Reynolds numbers*, Int. J. Numer. Methods Fluids **14** n° 9, 1992.

[5] T. Kawamura, H. Takami, K. Kuwahara, *New Higher-order upwind scheme for incompressible Navier-Stokes equations* , Lect. Notes Phys. **218**, 1985.

[6] K. Kuwahara, *Computational fluid dynamics and visualization: Cavity flow at Reynolds number* 100000, http://www2.icfd.co.jp

[7] B.P. Leonard, *The ULTIMATE conservative difference scheme applied to unsteady one-dimensional advection* , Comput. Methods Appl. Mech. Eng. **88** n° 1, 1991.

[8] A. Miranville, X. Wang, *Upper bound on the dimension of the attractor for nonhomogeneous Navier-Stokes equations*, Discrete Contin. Dynam. Systems **2** n° 1, 1996.